Optical and Quantum Electronics (2022) 54:721
https://doi.org/10.1007/s11082-022-03970-8

Analysis of femtosecond microstructured Poly Lactic Acid temporary cell scaffolds, spin-coated with Chitosan or Hydroxyapatite

L. Angelova[1] · A. Daskalova[1] · E. Filipov[1] · R. Mincheva[2] · X. Carette[2] · D. Miano[3] · D. Aceti[1] · A. Trifonov[4] · I. Buchvarov[4]

Received: 12 October 2021 / Accepted: 5 July 2022 / Published online: 15 September 2022

Abstract
Temporary biocompatible and degradable cell scaffolds - the new weapon of tissue engineering in the face of personalized medicine are emerging as one of the most powerful tools for guided self-regeneration of injured, diseased or malfunctioning tissues. In the current study, CPA Ti:sapphire fs laser system ($\tau = 150$ fs, $\lambda = 800$ nm, $\nu = 0.5$ kHz) was used for surface modification of Poly Lactic Acid (PLA) temporary cell scaffolds at fluence $F = 0.8$ J/cm^2 and scanning velocity $V = 3.8$ mm/s. Additional thin layer of chitosan (Ch)/hydroxyapatite (HAp) (up to $30 \div 60$ nm thickness) was deposited on the laser-modified PLA matrices by spin coating method for cell scaffolds surface functionalization. In order to observe the complementary impact of fs structuring and spin coating on the PLA scaffolds' properties, both surface modification methods were applied on the prepared by compression molding PLA samples. Each laser processed sample was analyzed in respect of the corresponding control – laser-treated and untreated PLA surface, spin-coated with Ch or HAp. The microstructured scaffolds were characterized by SEM, EDX, FTIR, roughness, and WCA analyses. The results obtained from characterization of scaffold properties, show that such combined methods application for functionalization of the bone PLA scaffolds could be applied to improve the biocompatibility of the as created PLA-chitosan and PLA- hydroxyapatite hybrid cell matrices.

Keywords Biopolymer cell scaffolds · Femtosecond laser modification · Spin coating · Bone tissue engineering · Temporary cell matrices

This article is part of the Topical Collection on Photonics: Current Challenges and Emerging Applications, Guest edited by Jelena Radovanovic, Dragan Indjin, Maja Nesic, Nikola Vukovic and Milena Milosevic.

Extended author information available on the last page of the article

1 Introduction

Nowadays, tissue engineering is emerging as an increasingly preferred choice for the regeneration of irreversible bone tissue defects. Temporary cell scaffolds, based on degradable and biocompatible biopolymers are one of the most powerful tools for guided self-regeneration of injured, diseased or malfunctioning tissues (Hutmacher et al. 2007; Scheinpflug et al. 2018; Bose et al. 2012). Apart from permanent implants, the transplantation of bone tissue is extremely limited by donor shortage (Olson et al. 2011). These cell environmental structures, on the other hand, could serve as mechanically stable, supporting platforms for the patient's own cells attachment and proliferation. The scaffolds are gradually being displaced by the newly formed bone tissue in an absolutely natural way (Scheinpflug et al. 2018; Alaribe et al. 2016), without a development of an immune response (Dahlan et al. 2012; Mukherjee 2014; Derakhshanfar et al. 2018; Wua et al. 2014).

In recent years scientists are in constant search and optimization of the best materials for restoring, maintaining, and improving cell scaffold function. In particular, their biocompatibility and "extracellular matrix qualities", such as surface roughness, wettability, hierarchical interconnected porosity, anti-inflammatory properties, etc. Above all, the optimal cellular conditions should be accomplished without introducing additional cellular cytotoxicity changes in the chemical composition of the matrix structural materials (Saito et al. 2015; Stevens et al. 2008). The optimal solution is combining the qualities of precisely selected materials in certain quantitative ratios – for example, the elasticity and plasticity of polymers with the mechanical stability and hardness of ceramics (Wang et al. 2013). In order to fulfill the cell's viability needs, additional functionalization of the temporary cell platforms is an absolute requirement (Terakawa 2018; Krüger and Kautek 2004). Different (mostly chemical) methods for the structuring of temporal cell implants exist – fiber bonding, solvent casting, gas foaming, phase separation, electrospinning, etc. Most of them, unfortunately lead to irreversible and/or in many cases cytotoxic chemical alterations (O'Brien et al. 2015; Sears et al. 2016).

Femtosecond (fs) laser surface modification, on the other hand, is a non-thermal and precisely controlled cell scaffold optimization technique (Narayan et al. 2007; Terakawa 2018). This method does not change the chemical composition of the material in contrast it finely tunes topography properties, like wettability, charge, structuring, and porosity (Mukherjee et al. 2014; Govindarajan et al. 2014). Thus, an opportunity for precise optimization of the of the scaffold properties in respect to the concrete cell line seeding is provided. Femtosecond laser interaction with biological materials and tissues leads to minimal side effects, like microcracks formation, minimal heat diffusion in the interaction zone, absence of molten zones, and reduced ablation thresholds. This leads to ability of precise control over the biomaterials characteristics like porosity, surface roughness, wettability, etc. The proposed modification method could achieve strictly controlled porosity, which is crucial for normal cell functionalization. For example, the natural structure of bones possesses various types of pores with different dimensions - in the range of 1 μm - interaction with proteins; 1 μm÷20 μm participating in cell growth; 100 μm and up to more than 500 μm -for cell expansion and overall bone growth (Scheinpflug et al. 2018).

Due to its biocompatibility, biodegradability, mechanical stability, and strength, poly-lactic acid (PLA) is gradually being established as one of the basic biomaterials in the design of temporary tissue-engineered bone cell matrices (Santoro et al. 2016; Rasal et al. 2010). It

is a thermoplastic polyester of lactic acid, a natural non-toxic metabolic product, subject to the Carboxylic acid degradation pathway in the body (Serra et al. 2013). For example, the group of Lou et al. successfully fabricated nanocomposite scaffolds of poly(l-lactic acid)/β-tricalcium phosphate (PLLA/β-TCP) with three levels of hierarchical porosity, which supported MG-63 osteoblast cell line proliferation, penetration, and ECM deposition (Lou et al. 2014). The group of Li et al. demonstrated the femtosecond laser generation of controllable 3-D microchannels on (poly(l-lactide-co-ε-caprolactone)) copolymer scaffold that can induce specific myogenic differentiation of hMSCs (human mesenchymal stem cells) in vitro, even without additional functionalization of the cell matrix with biological factors (Li et al. 2012). The study of Lee and coauthors proved that fs laser processing can be used to increase cell infiltration into 3D electrospun nanofibrous poly(l-lactide) scaffolds and at the same time facilitates endothelial cell ingrowth (Lee et al. 2012). Yada and Terakawa for example were indeed able to generate laser-induced periodic surface structures (LIPSS) on the surface of poly-L-lactic acid scaffold by femtosecond laser structuring (Yada and Terakawa 2015). These nanostructures are well known for controlling cellular dynamics and adjust the biocompatible matrices to possess better bioactivity behavior.

In addition, chitosan (Ch) is a natural biocompatible, non-toxic, biofunctional, and hydrophilic polysaccharide, characterized by high antimicrobial activity and superior affinity to cell proteins (Arca et al. 2008; Martino et al. 2005; Muzzarelli 2011). These properties makes it a promising cell adhesion, non-inflammatory biomaterial (Suh and Matthew 2000; Hutmacher et al. 2001), that could serve as a bio-interface between the temporal implant and the healthy recipient tissue. In that way it can enhance bone formation both in vitro and in vivo, due to its good osteoconductive properties (Muzzarelli et al. 1994; Logith Kumar et al. 2016). For example, the group of Castillejo et al. reported successful cell culture on ns laser generated foam structures in chitosan samples (Castillejo et al. 2012).

Hydroxyapatite (HAp) is the form in which calcium phosphate is naturally found in bones - approx. 60% of the bone matrix is formed from this composition (Rho et al. 1998). The $Ca_{10}(PO_4)_6(OH)_2$ is known for its osteoconductive properties, a distinct condition which is absent in the PLA matrix, due to hydrophobic nature of the material (Serra et al. 2013). HAp is crucial for normal bone functioning and is a key component in the implant's "bonding glue" with surrounding tissues (Milella et al. 2001), as it makes a strong connection with them and enhances the mechanical properties of the cell scaffolds (Meskinfam et al. 2018). The group of Zhou et al., for example, showed that the addition of Ch and HAp to PLA scaffolds leads to enhanced adhesion, proliferation and differentiation, mineralization, and expression of esteogenic genes of MC3T3-E1 osteoblastic cell line (Zhou et al. 2017).

In the current study, CPA Ti:sapphire ultra-short laser system ($\tau = 150$ fs, $\lambda = 800$ nm, $v = 0.5$ kHz) was used for surface modification of 2D PLA samples at fluence $F = 0.8$ J/cm^2 and scanning velocity $V = 3.8$ mm/s. The additional thin layer of chitosan (Ch)/ hydroxyapatite (HAp) (up to $30 \div 60$ nm) was deposited on the laser processed PLA matrices by spin coating method for additional surface functionalization. The effect of ultra-short laser based patterning in combination with in situ spin coating layer deposition on compression molded PLA scaffolds were monitored.

The laser processed PLA scaffold was analyzed with respect to the corresponding control–laser-treated/untreated samples; Ch/Hap spin-coated, respectively. The microstructured scaffolds were investigated by Scanning Electron Microscopy (SEM), Energy Dispersive X-Ray analysis (EDX), Fourier transform infrared analysis (FTIR), profilometer, and water

contact angle (WCA) analyses. Based on the literature survey, and the obtained results from scaffolds characterization, an assumption could be made that such combined methods could represent a model for biomaterial functionalization.

2 Materials and methods

For the experimental needs 2D cell scaffolds of PLA were prepared via Carver 4122 12-12 H Manual Heated Press (Carver Inc., USA) by the method of compression molding (Fig. 1.1). The PLA granules (PLA 4060D, Nature Works, Nebraska, USA) were dried overnight/60°C in a vacuum and molded via the following procedure − 3 min/180°C, degassed in several cycles, 2 min/12 bars. The molded 2D PLA (thickness ~ 230 μm) was cut into 1 × 1 cm samples. Femtosecond laser functionalization of scaffolds surface (Fig. 1.2) was performed in the air via an amplified Ti: Sapphire laser system (Quantronix- Integra-C, Hamden, CT, USA) - central wavelength $\lambda = 800$ nm, $\tau = 150$ fs pulse duration, repetition rate $\nu = 0.5$ kHz, fluence $F = 0.8$ J/cm^2 and scanning velocity $V = 3.8$ mm/s (continuous scanning). The 2D molded PLA samples were patterned with parallel stripes with precisely defined dimensions and distance from each other, by moving vertically the motorized XYZ translation stage, on which the samples were positioned perpendicular to the laser beam. The precise control of the laser texturing was monitored by LabView software. The processed PLA scaffolds were analyzed in comparison to control PLA matrix.

For additional functionalization of the created PLA cell matrices a spin coater purchased from CaLCTec s.r.l., Calabria, Italy. It was used for covering the control PLA (cPLA) and fs laser processed PLA samples (fsPLA) with nm layer (up to 30 ÷ 60 nm) of Chitosan (cPLA-Ch and fsPLA-Ch) or Hydroxyappatite (cPLA-HAp and fsPLA-HAp) and were analyzed in relation to uncovered PLA scaffolds (cPLA and fsPLA). The protocols for Ch and HAp solutions preparation, used for the process are described elsewhere (Daskalova et al. 2019). Spin coating (Fig. 1.3) was performed twice on each sample with parameters given in Table 1. In each round, 1μL of the spin coating solution (Ch or HAp) was deposited on the 1 × 1 cm PLA plates by micropipette (Dlab, Beijing, China ISO9001/13,485 certified − 0.1–10μL) - coating with static rotation. The spin coater was then activated and rotation started - the centrifugal movement spread the solution on the sample, creating the substrate (spin up and off phases). The thinning and evaporation phase of the HAp/Ch nm film is the last step of the process. The rotation parameters of the spin coating were chosen based on the calibration curve for the used centrifuge movement. A schematic illustration of the main steps of synthesis and functionalization of the 2D PLA scaffolds is given in Fig. 1.

The surface morphology and elemental composition of obtained PLA plates were analyzed by a Scanning Electron Microscope SEM-TESCAN/LYRA/XMU (TESCAN ORSAY HOLDING, a.s., Brno, Czech Republic), equipped with an Energy Dispersive X-ray module (EDX Quantax 200, Bruker). The samples were carbon-coated (~10nm) in vacuum via a carbon sputtering system (Quorum Technologies) and images were taken at 100x ÷ 1000x magnification at a voltage of 20 kV. The corresponding elemental composition [wt.%] was defined at an operational voltage of 10 kV. 2D roughness of the examined PLA samples was evaluated by „TESA Rugosurf 10-10G" profilometer (ISO4287/JISB0601), working with a diamond needle ($\lambda_{cutoff} = 0.80$ mm and $n_{cutoff} = 5$). The R_a roughness parameter (representing the mean value of the deviations of the surface height from the median line, according to

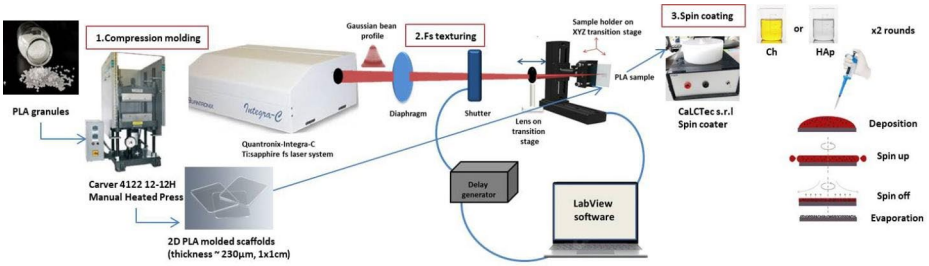

Fig. 1 Schematic illustration of the main experimental steps: (1) Compression molding of the row PLA granules; (2) Femtosecond laser microstructuring of the 2D PLA scaffolds; (3) Spin coating of the textured and control PLA samples with Ch /HAp nm layer, respectively, and main steps of the process

Table. 1 Spin coating parameters used for 1st and 2nd round of the PLA scaffolds spin coating

Spin coating	1st round	2nd round
Voltage (V)	8	10
Spinning velocity (rpm)	2500	3000
Time (s)	60	60

DIN4776 standards) was obtained as an average value over 5 separate measurements. For obtaining the IR transmittance spectra [%] of the PLA samples Fourier-Transform Infrared (FTIR) spectrophotometer (IR Affinity-1, Shimadzu, Kyoto, Japan), with a working range of 4500 − 500 cm^{-1} and resolution of 4 cm^{-1} was used for evaluation of possible chemical bonds alterations after laser treatment and detecting the presence of the Ch/HAp thin layers, applied on the relevant scaffolds. Water contact angle (WCA) evaluation of each sample was performed by homemade laboratory installation in the air with 1μL volume of dH_2O drop positioned perpendicular and in parallel to the laser created rows. The measurements were taken for a 7s duration period in intervals of 0.5s. The samples, fixed on a high-precision XYZ translation stage were dropped by a micropipette (Dlab, Beijing, China ISO9001/13,485 certified − 0.1–10 μL). The results obtained were processed by ImageJ software equipped with a contact angle plug-in - every WCA value was averaged over 10 separate measurements.

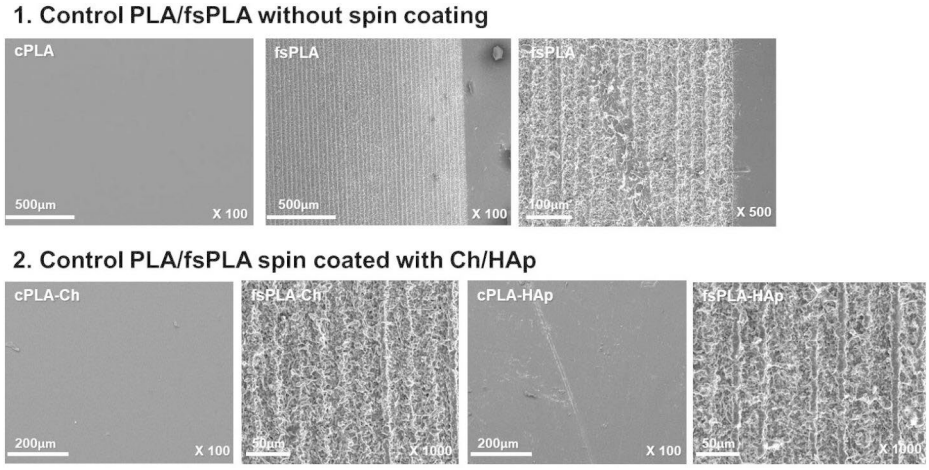

Fig. 2 SEM images of the 2D PLA scaffolds (magnification 100x÷1000x): (1) cPLA/fsPLA without a spin coating; (2) cPLA / fsPLA spin - coated with Ch/HAp

3 Results and discussion

3.1 SEM and EDX analysis of 2D PLA scaffolds

SEM images presented in Fig. 2 revealed a clear difference in the morphology of the processed /non processed PLA samples, while no morphological difference was monitored when Ch/HAp coating was applied in relation to the corresponding control sample, even at the SEM images with the highest magnification.

The femtosecond laser structuring led to porous groove formation along the PLA surface. Clear edges and no damage in the scaffold surface structure (without molten zones) were monitored; the roughness parameter was measured to be Ra_{fsPLA}=1.92 µm. The corresponding value of the control visually smooth, non-processed surface is Ra_{cPLA}=0.2. The surface roughness, created by the laser texturing in comparison to the depth (6.3 µm) and width (1.2 µm) of the created grooves, is in line with the optimal range for seeding of MSCs in respect to their dimensions (Ra = 0.9 ÷ 1.53 µm) proved by Szmukler-Moncler et al. (Szmukler-Moncler et al. 2004). This observation leads to successful MSCs orientation along the porous structures, as already reported in a previous study by our research group (Daskalova et al. 2021). Furthermore, the additionally deposited nm layer of Ch/HAp, by spin coating, in the range of ~ 30 ÷ 60 nm, indicated no change in the overall roughness of the observed samples (Fig. 3). Thus, we hypothesize, based on previously obtained results (Daskalova et al. 2021), that additional surface functionalization with Ch/Hap could affect cellular behavior.

The corresponding results of the performed EDX analysis are presented in Fig. 4 (EDX spectra), and Table 2 - EDX [wt%] elemental concentration of the elements of interest C, O; Ca, and P (for HAp spin-coated samples).

The acquired EDX spectra from all samples do not reveal presence of uncommon elements for the examined PLA matrix, only deviations in the [wt%] elemental concentrations can be observed (Table 2). Femtosecond laser modification of the 2D scaffolds leads

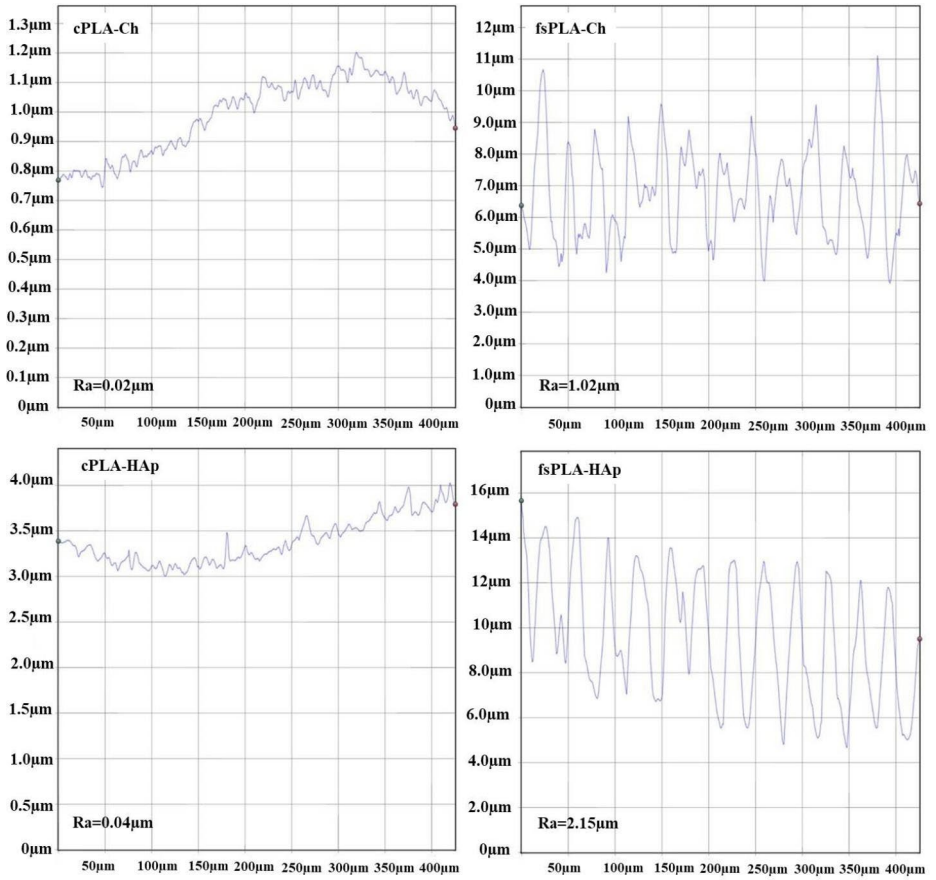

Fig. 3 R_a-line roughness cross-section profile of control and laser-processed PLA samples, after spin-coated with Ch or HAp. The corresponding averaged Ra values are given for each sample

to lower values of C [wt%] and higher values of O [wt%] concentration, in comparison to the control surface of the corresponding sample (cPLA, cPLA-Ch, cPLA-HAp). These observations could be attributed to the breakage of side O-C = O chemical bonds of the PLA backbone leading to surface oxidation. In contrast, as expected, the [Ca] and [P] are detected only in the HAp coated samples (Figs. 4, 5 and 6; Table 2). Moreover, as can be seen from the results, hydroxyapatite accumulates selectively on laser modified zones. It is detected 5 to 7 times higher [wt%] of Ca and P on laser modified PLA samples in relation to cPLA-HAp. As general, this effect could be crucial for improving the PLA matrix implantation, and uptake in the body, since HAp is a key component in implants and serves as a "bonding material" with surrounding tissues (Milella et al. 2001).

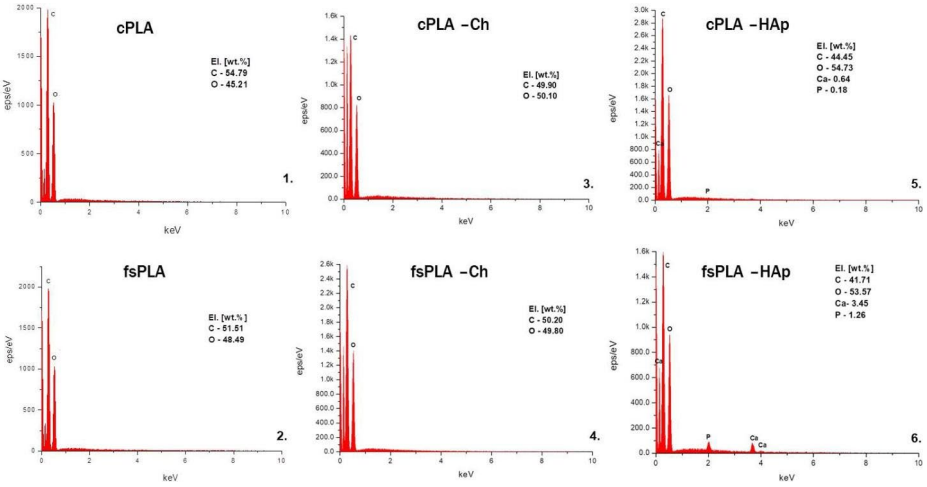

Fig. 4 EDX spectra of the PLA samples examined, as follows: (1) cPLA; (2) fsPLA; (3) cPLA-Ch; (4) fsPLA-Ch; (5) cPLA-HAp; (6) fsPLA-HAp

Table. 2 EDX [wt%] elemental concentration of the 2D PLA scaffolds examined. The detected P and Ca [wt%] in the HAp spin-coated PLA samples are determined and marked by colour

Sample	C [wt.%]	O [wt.%]	Ca [wt.%]	P [wt.%]
cPLA	54.79	45.21	-	-
fsPLA	51.51	48.49	-	-
cPLA-Ch	49.90	50.10	-	-
fsPLA-Ch	50.20	49.80	-	-
cPLA-HA	44.45	54.73	0.64	0.18
fsPLA-HA	41.71	53.57	3.45	1.26

3.2 FTIR analysis of examined PLA plates

FTIR spectroscopy was performed to evaluate the chemical composition of the PLA scaffolds (Fig. 5). The characteristic chemical bonds of PLA, Ch, and HAp detected by the FTIR spectroscopy are given in Table 3.

As can be seen from the presented FTIR spectra, all characteristic transmittance bands of PLA, Ch, and HAp are observed from the corresponding samples. The only obvious difference is in the intensity of the PLA peaks, after femtosecond laser structuring, without shift in their position (Figs. 5 – 1). The characteristic PLA bands obtained from the examined samples (Figs. 5 – 1 and 2) are as follows: 3750 cm^{-1}, (O–H bond stretching), 2925 cm^{-1} (resonance of side CH_3 groups), 1747 cm^{-1} (C = O stretching), 1182 cm^{-1} (C–O–C stretch-

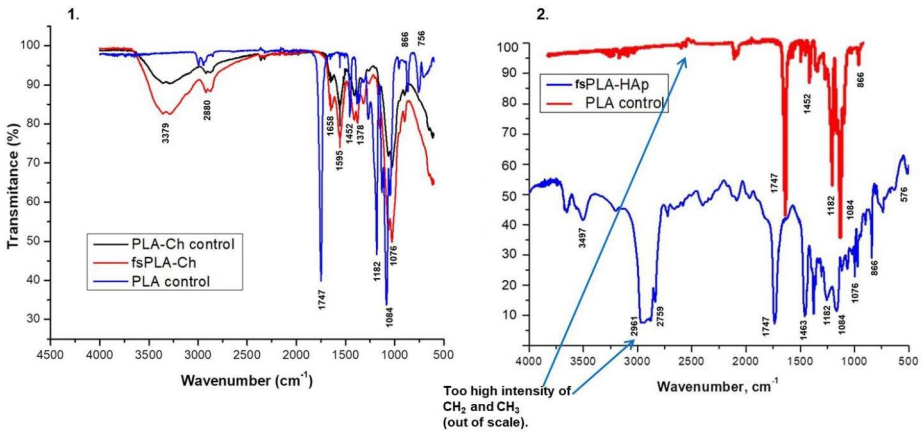

Fig. 5 FTIR transmittance spectra of: (1) Ch spin-coated PLA samples, compared to control PLA; (2) HAp spin-coated fsPLA, compared to a control sample

ing), 1452 cm^{-1} (carbonyl resonance) and 1084 cm^{-1} (COOH) (Lasprilla et al. 2012). Apart from PLA, the transmittance spectra of cPLA-Ch and fsPLA-Ch (Figs. 5−1) reveal clearly strong presence of chitosan traces in the spin-coated scaffolds. The well-defined maximum at 3379 cm^{-1}, corresponds to O–H bond stretching in the chitosan molecule. The band at 2880 cm^{-1} is attributed to C-H stretching, while the peaks at 1595 and 1658 cm^{-1} are due to N-H bond stretching. The peak of the O bridge stretching is detected at 1378 cm^{-1} and the C-H stretching in Ch molecules is detected at 1076 cm^{-1}. All characteristic transmittance bands of the chitosan, reported in the current study, are in accordance with the FTIR spectra of pure Chitosan (Shajahan et al. 2014).

The transmittance spectra of HAp spin-coated fsPLA scaffold, in comparison to the cPLA sample, are presented in Figs. 5−2. The FTIR spectroscopy of the cPLA-HAp did not reveal the presence of HAp, due to the extremely low quantity of HAp (up to 7 x lower) deposited on the surface of non- modified PLA, which is in agreement with the EDX results presented in Figs. 4 and 5; Table 2. However, the presence of hydroxyapatite layer on the surface of the fsPLA spin-coated sample (Figs. 5−2) is detected, although the intensity of the transmittance spectra of its characteristic bands (Table 3) is significantly lower than that of the PLA matrix underlying it – 1747, 1182 and 1084 cm^{-1} peaks are clearly expressed. The band detected around~2925 cm^{-1}, and attributed to CH groups of PLA, is with too high intensity in relation to the fsPLA-HAp spectrum (Figs. 5−2). Apart from the appearance of typical PLA transmittance bands, characteristic bands of HAp are clearly defined. The transmittance band at 3497 cm^{-1} corresponds to O-H stretching, while that at 1463 cm^{-1} is attributed to the typical CO_2 absorption by the HAp molecules. A strong indication of the hydroxyapatite presence are expressed by the presence of peaks detected at 1056 and 578 cm^{-1}, which represent the PO_4 asymmetric and n4 symmetric P-O vibration stretching of PO_4, respectively (Rocha et al. 2005; Varma and Babu 2005).

	Hydroxyapatite					Chitosan					PLA				
Band (cm^{-1})	578	1056	1463	2759-2961	3497	1076	1378	1595 and 1658	2880	3379	1084	1182	1747	2925	3750
Group	PO_4 asymmetric stretching	PO_4 n4 symmetric stretching	CO_3 absorption	C-H stretching	O-H stretching	C-O stretching	bridge O stretching	N-H stretching	C-H stretching	O-H stretching	COOH	C–O–C stretching	C=O stretching	CH_3	O-H stretching

Table. 3 Chemical bonds detected in PLA (green), Ch (yellow), and HAp (blue) FTIR spectra at the corresponding transmittance band (cm^{-1})

3.3 WCA evaluation of the PLA samples

The WCA measurements were acquired in two directions for the femtosecond laser processed PLA samples – perpendicular and parallel to the laser-created grooves. The results presented in Figs. 6−1 and Figs. 6−2, for Ch and HAp spin-coated PLA scaffolds, respectively, in accordance to control samples (cPLA and fsPLA), reveal the hydrophobic nature of the unmodified PLA, WCA_{cPLA}=138.6°. The hydrophobicity of the PLA surface is one of its main disadvantages as temporal implant material (Alves et al. 2009). In contrast, femtosecond laser modification, enhances the wettability of PLA. It is monitored a decrease in WCA values to 52° for a time period of 7s, in the case of fsPLA.

As can be seen from Fig. 6, the WCA gradually decreases in accordance to time evolution, which is valid for all modification conditions presented in the current study. The observed effect could be explained by the homogeneous wetting effect on rough surfaces appearing when the water drop is in stable equilibrium (this phenomenon is valid, when minimum free energy of the system is achieved), described by the Wenzel model (Wenzel 1936). Spin coating with Ch and HAp leads to further enhancement of the hydrophilic properties of the PLA surface, especially when applied to laser modified scaffolds. It was evaluated a decrease of WCA values from 108.5° to 55.3° for chitosan spin-coated fsPLA. Similar observation was present for hydroxyapatite covered fsPLA (measured along the laser created grooves after a 7s period of application), where the WCA value decreased from 124° to 72.8°. The improvement of surface wettability, in combination with the surface roughness (Ra_{fsPLA}=1.92 µm), with no indication of chemical structure alterations, and the non-inflammatory and osteoconductive properties of chitosan or the surrounding tissue binding affinity of bone hydroxyapatite are all prerequisites that would lead to enhancement of cell adhesion on the designed PLA scaffolds, which is the basis for successful implant fabrication in tissue engineering. Therefore, cell viability studies and comparison of the results with the ones obtained on laser modified PLA without spin coating (Daskalova et al. 2021) are intended as a next step in our research. Moreover, fabrication and analysis of PLA scaffolds, spin-coated with hybrid Ch-HAp nm layers are also envisaged.

4 Conclusions

In this study, both surface modification methods described above were applied on PLA self-standing films. The main purpose of this study was to monitor their complementary impact on the scaffold's properties for optimized application in tissue engineering. The microstructured scaffolds were investigated by SEM, EDX, FTIR, profilometer, and WCA analyses. The presented experimental results clearly show, that the combined application of laser based structuring with the precise spin coating method leads to improved wettability, laser-enhanced surface roughness and porosity without chemical structure alterations,

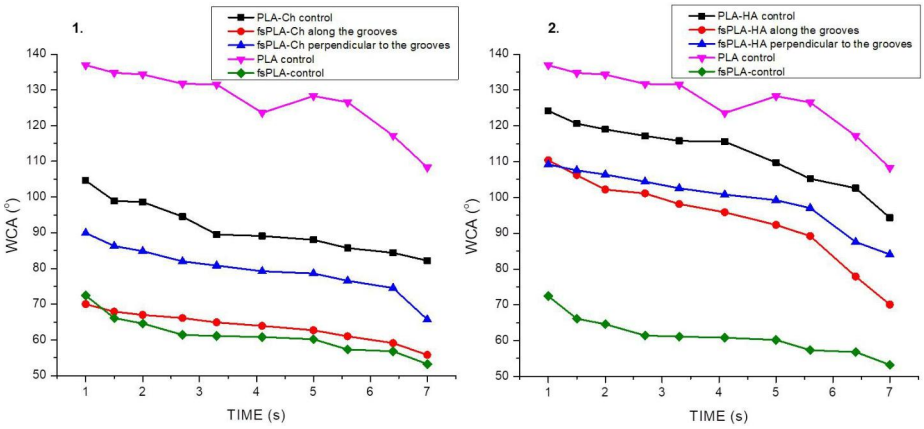

Fig. 6 WCA evaluation of: (1) Ch spin-coated and (2) HAp spin-coated PLA, compared to the corresponding controls

and even to several times improved deposition of HAp on laser-processed PLA scaffolds. Such combined functionalization of tissue scaffolds could essentially improve the bioactive properties of the created biomimetic hybrid matrices. As a next step, further biological evaluation and cell viability studies will be performed for investigating the influence over cellular dynamics. Monitoring the disordered spreading on smooth surfaces to a tendency of cell orientation and elongation along the laser created grooves (Daskalova et al. 2021), with respect to Ch/Hap effect on the cell's behavior is also planned. Spin coating with either of these biomaterials could additionally enhance femtosecond functionalization of the PLA matrices, and in that way could promote temporal bone implant improved integration in the recipient organism.

Supplementary Information The online version contains supplementary material available at https://doi.org/10.1007/s11082-022-03970-8.

Acknowledgements This research was funded by BULGARIAN NATIONAL SCIENCE FUND (NSF) under grant number No. KP-06-H48/6 (2020–2023), „Development of hybrid functional micro/nanoporous biomaterial scaffolds by ultra-fast laser modification"; EUROPEAN UNION'S H2020 research and innovation programme under the Marie Sklodowska-Curie Grant Agreement No. 861138 and H2020 FET Open METAFAST Grant Agreement No. 899673.

Declarations

The authors have no relevant financial or non-financial interests to disclose.

References

Alaribe, F.N., Manoto, S.L., Motaung, S.C.K.M.: Scaffolds from biomaterials: advantages and limitations in bone and tissue engineering. Biologia. 71, 353–366 (2016)

Alves, N.M., Shi, J., Oramas, E., Santos, J.L., Tomas, H., Mano, J.F.: Bioinspired superhydrophobic poly(L-lactic acid) surfaces control bone marrow derived cells adhesion and proliferation. J. Biomed. Mater. Res. A. 91, 480–488 (2009)

Arca, H., Şenel, S.: Chitosan Based Systems for Tissue Engineering Part 1: Hard Tissues. Fabad J. Pharm. Sci. 33, 35–49 (2008)
Bose, S., Roy, M., Bandyopadhyay, A.: Recent advances in bone tissue engineering scaffolds. Trends Biotechnol. 30, 546–554 (2012)
Dahlan, K., Dewi, S., Nurlaila, A., Soejoko, D.: Synthesis and Characterization of Calcium Phosphate/Chitosan Composites. Int. J. Bas Appl. Sci. 12, 50–57 (2012)
Daskalova, A., Angelova, L., Filipov, E., Aceti, D., Mincheva, R., Carrete, X., Kerdjoudj, H., Dubus, M., Chevrier, J., Trifonov, A., Buchvarov, I.: Biomimetic Hierarchical Structuring of PLA by Ultra-Short Laser Pulses for Processing of Tissue Engineered Matrices: Study of Cellular and Antibacterial Behavior. Polymers. 13, 2577 (2021)
Daskalova, A., Bliznakova, I., Angelova, L., Trifonov, A., Declercq, H., Buchvarov, I.: Femtosecond Laser Fabrication of Engineered Functional Surfaces Based on Biodegradable Polymer and Biopolymer/Ceramic Composite Thin Films. Polymers. 11, 378 (2019)
Derakhshanfar, S., Mbeleck, R., Xu, K., Zhang, X., Zhong, W., Xing, M.: 3D bioprinting for biomedical devices and tissue engineering: A review of recent trends and advances. Bioact Mat. 3, 144–156 (2018)
Govindarajan, T., Shandas, R.: A Survey of Surface Modification Techniques for Next-Generation Shape Memory Polymer Stent Devices. Polym. 6, 2309–2331 (2014)
Hutmacher, D.W., Schantz, J.T., Lam, C.X.F., Tan, K.C., Lim, T.C.: State of the art and future directions of scaffold-based bone engineering from a biomaterials perspective. J. Tissue Eng. Regener Med. 1, 245–260 (2007)
Hutmacher, D.W., Goh, J.C., Teoh, S.H.: An introduction to biodegradable materials for tissue engineering applications. Ann. Acad. Med. Singapore. 30, 183–191 (2001)
Krüger, J., Kautek, W.: Ultrashort pulse laser interaction with dielectrics and polymers. Adv. Polym. Sci. 168, 247–289 (2004)
Lasprilla, A.J.R., Martinez, G.A.R., Lunelli, B.H., Jardini, A.L., Filho, R.M.: Poly-lactic acid synthesis for application in biomedical devices—A review. Biotechnol. Adv. 30, 321–328 (2012)
Lee, B., Jeon, H., Wang, A., Yan, Z., Yu, J., Grigoropoulos, C., Li, S.: Femtosecond laser ablation enhances cell infiltration into three-dimensional electrospun scaffolds. Acta Biomater. 8, 2648–2658 (2012)
Li, H., Wen, F., Wong, Y.S., Boey, F.Y., Subbu, V.S., Leong, D.T., Ng, K.W., Ng, G.K., Tan, L.P.: Direct laser machining-induced topographic pattern promotes up-regulation of myogenic markers in human mesenchymal stem cells. Acta Biomater. 8, 531–539 (2012)
Logith Kumar, R., KeshavNarayan, A., Dhivya, S., Chawla, A., Saravanan, S., Selvamurugan, N.: A review of chitosan and its derivatives in bone tissue engineering. Carbohydr. Polym. 151, 172–188 (2016)
Lou, T., Wang, X., Song, G., Gu, Z., Yang, Z.: Fabrication of PLLA/βTCP nanocomposite scaffolds with hierarchical porosity for bone tissue engineering. Int. J. Biol. Macromol. 69, 464–470 (2014)
Martino, A.D., Sittinger, M., Risbud, M.V.: Chitosan: a versatile biopolymer for orthopaedic tissue-engineering. Biomaterials. 26, 5983–5990 (2005)
Meskinfam, M., Bertoldi, S., Albanese, N., Cerri, A., Tanzi, M.C., Imani, R., Baheiraei, N., Farokhi, M., Fare, S.: Polyurethane foam/nano hydroxyapatite composite as a suitable scaffold for bone tissue regeneration. Mater. Sci. Eng. C Mater. Biol. Appl. 82, 130–140 (2018)
Milella, E., Cosentino, F., Licciulli, A., Massaro, C.: Preparation and characterization of titania/hydroxyapatite composite coatings obtained by sol-gel process. Biomaterials. 22, 1425–1431 (2001)
Muzzarelli, R.A., Mattioli-Belmonte, M., Tietz, C., Biagini, R., Ferioli, G., Brunelli, M.A., et al.: Stimulatory effect on bone formation exerted by a modified chitosan. Biomaterials. 15, 1075–1081 (1994)
Muzzarelli, R.A.A.: Chitosan composites with inorganics, morphogenetic proteins and stem cells, for bone regeneration. Carbohydr. Polym. 83, 1433–1445 (2011)
Narayan, R.J., Jin, C., Doraiswamy, A., Mihailescu, I.N., Jelinek, M., Ovsianikov, A., Chichkov, B., Chrisey, D.B.: Laser processing of advanced bioceramics. Adv. Eng. Mater. 9, 83–83 (2007)
O'Brien, C., Holmes, B., Faucettm, S., Zhang, L.G.: 3D printing of nanomaterial scaffolds for complex tissue regeneration. Tissue Eng. B Rev. 21, 1–45 (2015)
Olson, J., Atala, A., Yoo, J.: Tissue Engineering: Current Strategies and Future Directions. Chonn Med. J. 47, 1–13 (2011)
Rasal, R.M., Hirt, D.E.: Poly(lactic acid) toughening with a better balance of properties. Macromol. Mater. Eng. 295, 204–209 (2010)
Rho, J.Y., Kuhn-Spearing, L., Zioupos, P.: Mechanical properties and the hierarchical structure of bone. Med. Eng. Phys. 20, 92–102 (1998)
Rocha, J.H.G., Lemos, A.F., Kannan, S., Agathopoulos, S., Ferreira, J.M.F.: Hydroxyapatite scaffolds hydrothermally grown from aragonitic cuttlefish bones. Journals of Materials Chemistry. 15, 5007–5011 (2005)
Saito, T., Teraoka, K., Ota, K.:Arrayed three-dimensional structures designed to induce and maintain a cell pattern by a topographical effect on cell behavior: Mater. Sci. Eng. C. 49, 256–261 (2015)

Santoro, M., Shah, S.R., Walker, J.L., Mikos, A.G.: Poly(lactic acid) nanofibrous scaffolds for tissue engineering. Adv. Drug Deliv Rev. 107, 206–212 (2016)
Scheinpflug, J., Pfeiffenberger, M., Damerau, A., Schwarz, F., Textor, M., Lang, A., Schulze, F.: Journey into Bone Models: A Review. Genes. 9, 247–283 (2018)
Sears, N.A., Seshadri, D.R., Dhavalikar, P.S., Cosgriff-Hernandez, E.: A Review of three-dimensional printing in tissue engineering. Tissue Eng. B Rev. 22, 298–310 (2016)
Serra, T., Mateos-Timoneda, M.A., Planell, J.A., Navarro, M.: 3D printed PLA-based scaffolds. Organogenesis. 9, 239–244 (2013)
Suh, J.K., Matthew, H.W.: Application of chitosan-based polysaccharide biomaterials in cartilage tissue engineering: a review. Biomaterials. 21, 2589–2598 (2000)
Stevens, B., Yang, Y.Z., Mohanda, S.A., Stucker, B., Nguyen, K.T.: A review of materials, fabrication to enhance bone regeneration in methods and strategies used engineered bone tissues. J. Biomed. Mater. Res. B. 85, 573–582 (2008)
Szmukler-Moncler, S., Perrin, D., Ahossi, V., Magnin, G., Bernard, J.P.: Biological properties of acid etched titanium implants: Effect of sandblasting on bone anchorage. J. Biomed. Mater. Res. B Appl. Biomater. 68, 149–159 (2004)
Terakawa, M.: Femtosecond laser processing of biodegradable polymers. Appl. Sci. 8, 1123 (2018)
Yada, S., Terakawa, M.: Femtosecond laser induced periodic surface structure on poly-L-lactic acid. Opt. Express. 23, 5694–5703 (2015)
Varma, H.K., Babu, S.: Synthesis of Calcium Phosphate Bioceramics by Citrate Gel Pyrolysis Method. Ceram. Int. 31, 109–114 (2005)
Wang, D.X., He, Y., Bi, L., Qu, Z.H., Zou, J.W., Pan, Z., Fan, J.J., Chen, L., Dong, X., Liu, X.N., et al.: Enhancing the bioactivity of poly (lactic-co-glycolic acid) scaffold with a nano-hydroxyapatite coating for the treatment of segmental bone defect in a rabbit model. Int. J. Nanomed. 8, 1855–1865 (2013)
Wenzel, R.N.: Resistance of solid surfaces to wetting by water. Ind. Eng. Chem. 28, 988 (1936)
Wua, S., Liu, X., Yeung, K., Liu, C., Yang, X.: Biomimetic porous scaffolds for bone tissue engineering. Mat. Sci. Eng. R. 80, 1–36 (2014)
Zhou, G., Liu, S., Ma, Y., Xu, W., Meng, W., Lin, X., Wang, W., Wang, S., Zhang, J.: Innovative biodegradable poly(L-lactide)/collagen/hydroxyapatite composite fibrous scaffolds promote osteoblastic proliferation and differentiation. Int. J. Nanomed. 12, 7577–7588 (2017)

Authors and Affiliations

L. Angelova[1] · A. Daskalova[1] · E. Filipov[1] · R. Mincheva[2] · X. Carette[2] · D. Miano[3] · D. Aceti[1] · A. Trifonov[4] · I. Buchvarov[4]

✉ L. Angelova
liliya_angelova@ie.bas.bg

I. Buchvarov
lily1986@abv.bg

[1] Institute of Electronics, Bulgarian Academy of Sciences, Sofia, Bulgaria

[2] Laboratory of Polymeric and Composite Materials (LPCM), University of Mons, Mons, Belgium

[3] Faculty of Physics, University of Calabria, Calabria, Italy

[4] Physics Department, Sofia University "St. Kliment Ohridski", Sofia, Bulgaria